



ISSN: 0067-2904

Milk Thistle Leaves Aqueous Extract as a New Corrosion Inhibitor for Aluminum Alloys in Alkaline Medium

Khudhair Abbas Kareem Al-Rudaini *, Khulood Abid Saleh Al-Saadie

Department of Chemistry, Collage of Since, University of Baghdad, Baghdad, Iraq

Received: 25/4/2020

Accepted: 19/6/2020

Abstract

The aqueous extract of milk thistle (*Silybum marianum*) leaves as a green corrosion inhibitor for AA7051 aluminum alloy in sodium hydroxide solution was investigated at a range of temperatures. Potentiodynamic polarization findings exhibit a mixed-type inhibitor with directly increased inhibition efficiency with the concentration of inhibitor. The adsorption of the inhibitor on aluminum alloy obeys Langmuir isotherm and the kinetic as well as thermodynamic parameters were measured and discussed.

Keywords: Aluminum alloy, milk thistle, Polarization, alkaline corrosion

المستخلص المائي لأوراق الكلغان كمثبط تآكل جديد لسبائك الالمنيوم في الوسط القاعدي

خضير عباس كريم الرديني*، خلود عبد صالح السعدي

قسم الكيمياء، كلية العلوم، جامعة بغداد، بغداد، العراق

الخلاصة

تم دراسة قابلية المستخلص المائي لأوراق الكلغان (*Silybum marianum*) على تثبيط تآكل سبيكة الالمنيوم المرقمة AA7051 في محلول هيدروكسيد الصوديوم على مدى من الدرجات الحرارية. أظهرت نتائج الاستقطاب الديناميكي ان المثبط من النوع المختلط وان كفاءة التثبيط تزداد بزيادة تركيز المثبط. كما وبينت الدراسة ان امتزاز المادة يتبع علاقة لانكماير و ان كل من المتغيرات الحركية و الترمودينمكية قد قيست و نوقشت.

1. Introduction

In the late 19th century, demand for aluminum was increased in the manufacturing of boats and cars, while the real revolution began in the early 20th century when it was used in aviation industry. However, aluminum applications in the second half of 20th century were not limited to its light weight but rather to corrosion resistance, electrical conductivity, thermal conductivity, easy fabrication, variable strength, and comparably cheap prices. Hence, the applications of aluminum in packaging, architecture, petroleum, and transportation were increased dramatically [1]. The contact of aluminum and aluminum alloy parts with alkaline solutions causes dissolution of the oxide layer that is naturally formed on aluminum surface and decreases corrosion resistance [2]. The corrosion can be eliminated be one of the following techniques: (i) development of new alloys that have more corrosion resistance in alkaline media; (ii) coating the aluminum with organic or inorganic coatings; (iii) inhibiting the corrosion with organic or inorganic inhibitors.

*Email: Khudhair.2010@yahoo.com

The applications of aluminum and its alloys restricted the type of techniques that can be used. First, the development of new alloy produces new properties that may not be suitable for certain applications; second, the coating is occasionally not ecofriendly or dissolved in concentrated alkaline; third, organic and inorganic inhibitors are either carcinogenic or expensive; and finally, the cost is an important factor, especially in industrial applications. These factors prompted researchers to find other methods that are appropriate to the industry's need.

The economic and ecofriendly inhibitors developed from plant extracts such as *Hibiscus sabdariffa* leaves[3], *Gossypium hirsutum* leaves[4], *Apium graveolens* seeds [5], *Sansevieria trifasciata* leaves [6], *Ambrosia maritime* leaves[7], sapota leaves [8], *Phyllanthus amarus* [9], and black acacia extract [10]. These plant extracts are utilized as green inhibitors for aluminum in alkaline medium with good corrosion efficiency, which prompts finding new inhibitors with higher efficiency and availability.

The present article investigated the water extract of milk thistle (*Silybum marianum*) as a novel green corrosion inhibitor for AA7051 aluminum alloy in sodium hydroxide solution and studied the electrochemical behavior of corrosion at a range of temperatures. In addition, kinetic and thermodynamic parameters were investigated in order to gain insight to the mechanism of inhibition.

2. Materials and methods

2.1. Sample preparation

The locally produced AA7051 aluminum alloy was cut to small pieces with 2.5cm diameter and polished with emery paper of 400 to 4000 mesh grid. The alloy was then washed by distilled water, put in ultrasonic bath with acetone, rinsed in distilled water, dried, and finally kept in a desiccator. The alloy type was confirmed by measuring X-ray fluorescence (XRF, XEPOS spectrometer, Germany) and the results in Figure-1 show the percentages of AA7051 aluminum alloy elements [11].

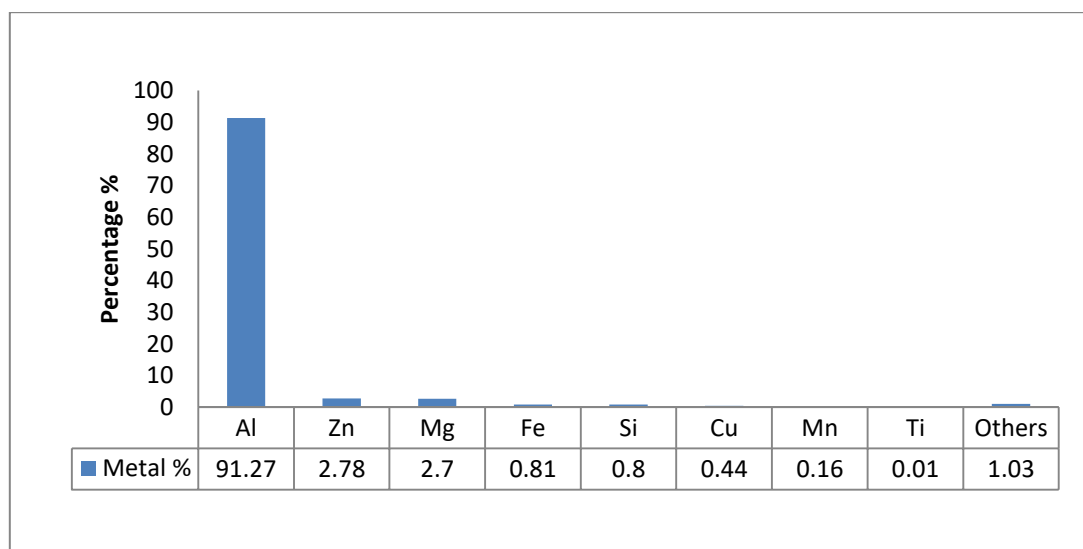


Figure 1-AA7051 aluminum alloy elements percentage

2.2. Extraction method

The leaves of milk thistle (ML) were collected from a house garden in Baghdad city, cut to small pieces, rinsed in tap water, dried for three days, ground in food processor, and sieved. The fine powder was placed in an extraction thimble of 500ml soxhlet extractor with distilled water and heated to 140°C for 7 hours. The extraction was transferred to a beaker and heated in an oven to evaporate the water, then the solid extraction was ground and kept in a closed flask for later use.

2.3. Electrochemical measurements

This electrochemical measurements were conducted by using potentiostat (Germany, MLab-2000) at 293, 303, 313, 323 and 333K with three-electrodes system of platinum (auxiliary sample), saturated calomel (reference sample), and aluminum alloy (working sample). The corrosion cell was filled with 1000mL of 0.01M sodium hydroxide with and without different amounts of extract (0.1, 0.2, 0.3, 0.4, 0.5g). After immersion in corrosive media for 15min, the open circuit potential (OCP) was measured

prior to polarization test. For each experiment the pH was measured by Hanna pH-meter (China) and kept around 12.

2.4. Surface characterization

The surface was characterized by Fourier transform infrared spectroscopy (FTIR) for the extract and the aluminum alloy sample immersed in alkaline solution containing the extract, after performing the corrosion test in the range of 400 to 4000 cm^{-1} by Shimadzu 8400S, Japan, spectrophotometer.

3. Results and discussion

3.1. Corrosion parameters

The corrosion parameters were calculated from Tafel plot by MLabSci software associated with the potentiostat and by Excel using the following equations [12,13]:

$$\text{IE}\% = \frac{I_{\text{corr}} - I_{\text{corr}}^{\text{inh}}}{I_{\text{corr}}} \times 100\% \quad (1)$$

$$R_p = \frac{I_{\text{corr}}}{2.303(b_a + b_c)I_{\text{corr}}} \quad (2)$$

where IE% is the inhibition efficiency, $I_{\text{corr}}^{\text{inh}}$ and

I_{corr} are currents of corrosion in presence and absence of inhibitor, respectively, R_p is polarization resistance ($\Omega \cdot \text{cm}^2$), and b_a and b_c are anodic and cathodic slopes, respectively. The data obtained are listed in Table-1.

Table 1-Electrochemical corrosion parameters for aluminum alloy in basic medium (pH=12) containing different concentrations of milk thistle extract at a range of temperatures.

C_{inh} (g/l)	T (K)	- OCP (mV)	$-E_{\text{corr}}$ (mV)	I_{corr} ($\mu\text{A}/\text{cm}^2$)	b_a (mv/Dec)	$-b_c$ (mv/Dec)	W.L ($\text{g}/\text{m}^2 \cdot \text{d}$ ay)	P.L (mm/year)	R_p ($\Omega \cdot \text{cm}^2$)	IE%	Θ
0.0	293	1237	1329.9	45.23	114.0	140.3	3.64	0.492	604.59	—	—
	303	1205	1255.2	84.85	209.3	377.1	6.83	0.923	689.68	—	—
	313	1209	1255.3	131.85	301.5	319.0	11.06	1.430	511.12	—	—
	323	1180	1166.3	150.38	280.8	362.7	11.21	1.640	457.59	—	—
	333	1198	1210.0	178.96	368.5	366.3	11.44	1.950	446.29	—	—
0.1	293	1343	1324.6	30.99	127.4	50.8	2.49	0.337	509.53	31.48	0.3148
	303	1296	1279.2	34.53	82.9	101.2	2.78	0.376	573.79	59.30	0.5930
	313	1255	1188.8	52.32	115.7	106.2	4.21	0.569	460.15	60.30	0.6030
	323	1216	1209.8	54.25	109.9	112.7	4.37	0.590	445.93	63.92	0.6392
	333	1185	1167.8	56.70	110.0	99.2	4.56	0.617	399.97	68.31	0.6831
0.2	293	1289	1281.7	26.56	100.7	72.7	2.14	0.289	691.12	41.27	0.4127
	303	1263	1264.5	25.97	62.6	54.6	2.09	0.283	488.24	69.39	0.6939
	313	1256	1238.4	34.10	83.2	51.9	2.74	0.371	407.52	74.13	0.7413
	323	1219	1211.6	38.27	88.9	73.6	3.08	0.416	457.44	74.55	0.7455
	333	1182	1188.4	46.53	81.9	70.4	3.74	0.506	353.74	73.99	0.7399
0.3	293	1392	1374.2	23.21	63.6	51.5	1.87	0.253	533.07	48.68	0.4868
	303	1286	1327.8	24.41	47.5	67.5	1.96	0.266	496.59	71.23	0.7123
	313	1232	1265.0	28.97	71.3	82.9	2.33	0.315	575.28	78.02	0.7802
	323	1230	1202.4	24.96	69.9	63.3	2.01	0.272	578.63	83.40	0.8340
	333	1185	1184.0	29.21	80.0	57.6	2.35	0.318	498.46	83.67	0.8367
0.4	293	1401	1392.8	19.67	50.1	53.7	1.58	0.214	572.90	56.51	0.5651
	303	1310	1309.0	17.52	48.7	26.7	1.41	0.191	427.96	79.35	0.7935
	313	1232	1125.9	19.52	58.1	49.5	1.57	0.212	595.33	85.19	0.8519
	323	1223	1216.6	19.29	49.8	43.0	1.55	0.210	520.10	87.17	0.8717
	333	1181	1179.2	11.36	50.5	36.1	0.915	0.124	805.70	93.65	0.9365
0.5	293	1370	1372.2	8.27	39.4	44.2	0.666	0.090	1095.1	81.71	0.8171
	303	1323	1306.4	13.42	25.8	37.3	1.08	0.146	494.10	84.18	0.8418
	313	1261	1264.3	13.64	24.1	36.4	1.10	0.148	462.19	89.65	0.8965
	323	1220	1223.2	9.47	24.4	25.4	0.762	0.103	571.36	93.70	0.9370
	333	1152	1152.4	17.90	31.8	30.2	1.44	0.195	376.23	89.99	0.8999

The data demonstrate a shift in open circuit potential (OCP) to more negative values with the addition of milk thistle extract. However, the open circuit potential was roughly independent upon the extract concentration. Furthermore, the addition of milk thistle extract considerably reduced the current of corrosion. This behavior shows its ability to prevent corrosion of aluminum alloy in NaOH medium [14]. The marginally dropped corrosion potential and dramatically increased corrosion current with increasing temperature are due to the increase in the rate of chemical dissolution of aluminum surface with temperature. In the same way, the weight loss (W.L) and penetration loss (P.L) were increased. After adding the inhibitor, the rate of corrosion was decreased and attained high inhibiting efficiency at 0.5g/L concentration of inhibitor.

3.2. Adsorption studies

In order to understand the mechanism of interaction of the inhibitor with metal surface and to calculate the thermodynamics adsorption parameters, surface coverage was calculated from the current of corrosion in the presence (I_{corr}^{inh}) and absence (I_{corr}) of inhibitor, using the following equation [15]:

$$\Theta = 1 - \left(\frac{I_{corr}^{inh}}{I_{corr}} \right) \quad (3)$$

The surface coverage Θ and inhibitor concentrations C_{inh} were substituted in Langmuir, Freundlich, and Temkin isotherms and the best fit with Langmuir isotherm was calculated by the following equation [16]:

$$\frac{C_{inh}}{\Theta} = \frac{1}{K_{ads}} + C_{inh} \quad (4)$$

where K_{ads} is the equilibrium constant of adsorption obtained from the plot of C_{inh} against $\frac{C_{inh}}{\Theta}$. As shown in Figure-2, the linear correlation ($R^2 > 0.98$) assumes that the adsorption of milk thistle on the aluminum alloy agreed with this isotherm. Langmuir model suggests a uniform surface with no interactions between adsorbed molecules [17]. The thermodynamic parameters of adsorption were calculated by using the following equations [15,18]:

$$\Delta G_{ads} = -2.303RT \log (55.5K_{ads}) \quad (5)$$

$$\log K_{ads} = \frac{-\Delta H_{ads}}{2.303RT} + \frac{\Delta S_{ads}}{2.303R} + \log \frac{1}{55.5} \quad (6)$$

where T (K) is the absolute temperature, R is the gas constant ($8.314 \text{ J.mol}^{-1}.\text{K}^{-1}$), 55.5 is the concentration of water in the molar unit, and ΔG_{ads} is the free energy of adsorption, ΔH_{ads} is the standard adsorption enthalpy calculated from the slope of $\log K_{ads}$ versus $1000/T$ (Figure-3) and from the intercept ΔS_{ads} standard entropy of adsorption calculated. The thermodynamic data represented in Table-2 refer to a spontaneous process of chemical adsorption on aluminum surface. The positive values of ΔH_{ads} and ΔS_{ads} indicate an endothermic process which interpreted the increase of inhibition efficiency with the temperature and the increase of entropy of adsorption [19].

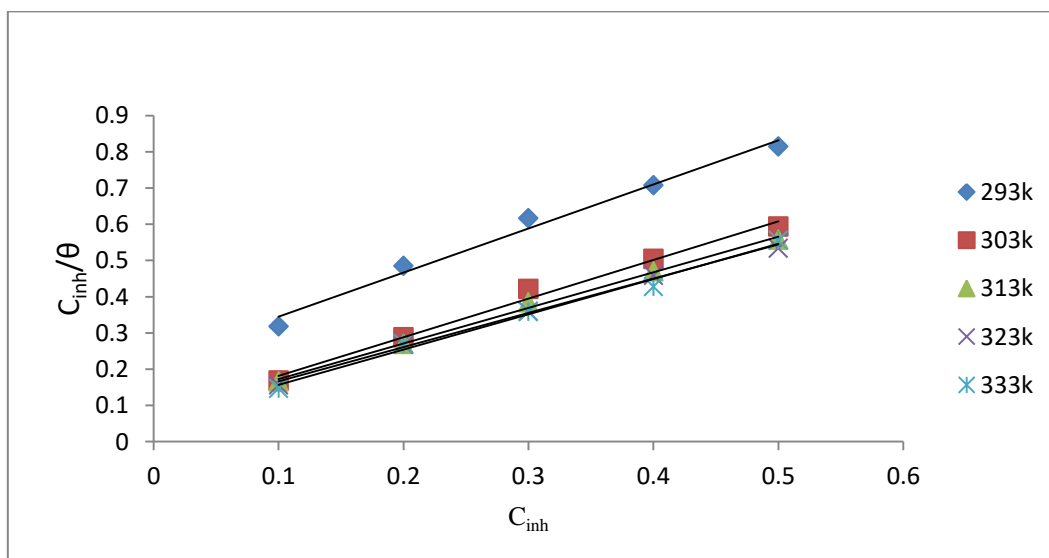


Figure 1-Langmuir's adsorption isotherms of ML on 7051 aluminum alloy in 0.01M NaOH.

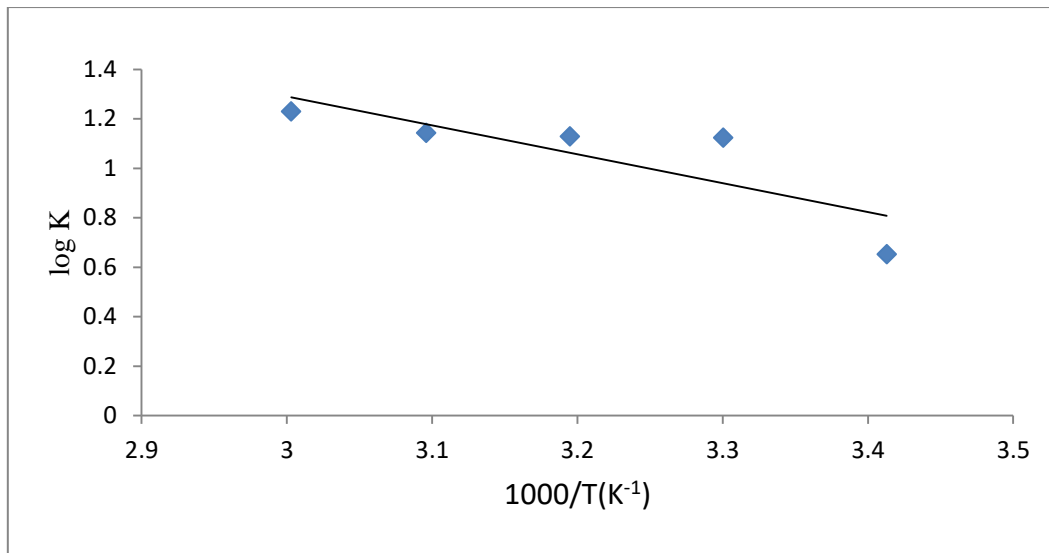


Figure 2-Straight line of log K versus 1000/T for 7051 aluminum alloy in 0.01M NaOH in presence and absence of ML extract

Table 2-Thermodynamic values of ML on 7051 aluminum alloy in 0.01 M NaOH

T(K)	ΔG_{ad} (kJ.mol ⁻¹)	ΔH_{ads} (kJ.mol ⁻¹)	ΔS_{ads} (J.mol ⁻¹ .K ⁻¹)
293	-13.439	26.41	125.36
303	-16.636		
313	-17.2164		
323	-17.8582		
333	-18.9587		

3.3. Kinetics of corrosion

The influence of temperature upon corrosion behaviors of the 7051 aluminum alloy in 0.01M NaOH, in presence and absence of various concentrations of milk thistle extract was examined at a range of temperatures of 293–333K, using polarization measurements (Figure-4). The relative kinetic parameters are listed in Table-3. The findings indicate that the rates of the 7051 aluminum alloy corrosion, in non-inhibited and inhibited alkaline solutions, rose linearly with temperature due to the increase in passive film dissolution [20]. Nevertheless, Figure-5 exhibits the increase in inhibition efficiency with increasing temperature, which evidently confirms the effectiveness of milk thistle extract as corrosion inhibitor in the range of temperature of this investigation. The energy of activation for the corrosion process was calculated by using the following natural logarithm form of Arrhenius equation [21]:

$$\ln I_{corr} = \ln A - \frac{E_a}{RT} \quad (7)$$

where I_{corr} is the current density of corrosion, A is the Arrhenius pre-exponential factor, and E_a is the apparent activation energy of the corrosion reaction. The apparent activation energy of the non-inhibited and inhibited corrosion reactions was determined from the slope of the linear plot of $\ln I_{corr}$ versus $1/T$ (Figure-6). The E_a values obtained are listed in Table-3 and exhibit that the E_a values of aluminum alloy in alkaline solutions with milk thistle extract are lower than those of the alkaline solutions without milk thistle extract. The decline in the apparent activation energy values for alkaline solutions containing milk thistle extract compared with pure alkaline solutions, in addition to the noticeable increase in the efficiency of inhibition with the increase of temperature, assume that few milk thistle components would be chemisorbed on the aluminum surface [22]. The activation parameters were calculated using Eyring transition state equation [23]:

$$I_{corr} = \frac{kT}{h} \exp\left(\frac{\Delta S^*}{R}\right) \exp\left(-\frac{\Delta H^*}{RT}\right) \quad (8)$$

where k is Boltzmann constant, R is gas constant (8.314 J.mol⁻¹.K⁻¹), h is Planck constant, ΔS^* is the activation entropy, and ΔH^* is the activation enthalpy [24]. From the plot of $\ln(I_{corr}/T)$ versus $1/T$ in Figure-7, the ΔH^* and ΔS^* values were calculated from the slope ($-\Delta H^*/R$) and the intercept ($\ln(R/N_A h) + (\frac{\Delta S^*}{R})$), respectively, and the observed data are listed in Table-3. The ΔH^* values carry

positive signs, referring to mild endothermic dissolution reaction of aluminum under the conditions of this investigation [25]. The large negative values of activation entropy in the presence and absence of milk thistle extract exhibited that the activated complex in the rate-determining step denotes association instead of dissociation and that the disorder of the activated complex is reduced [26].

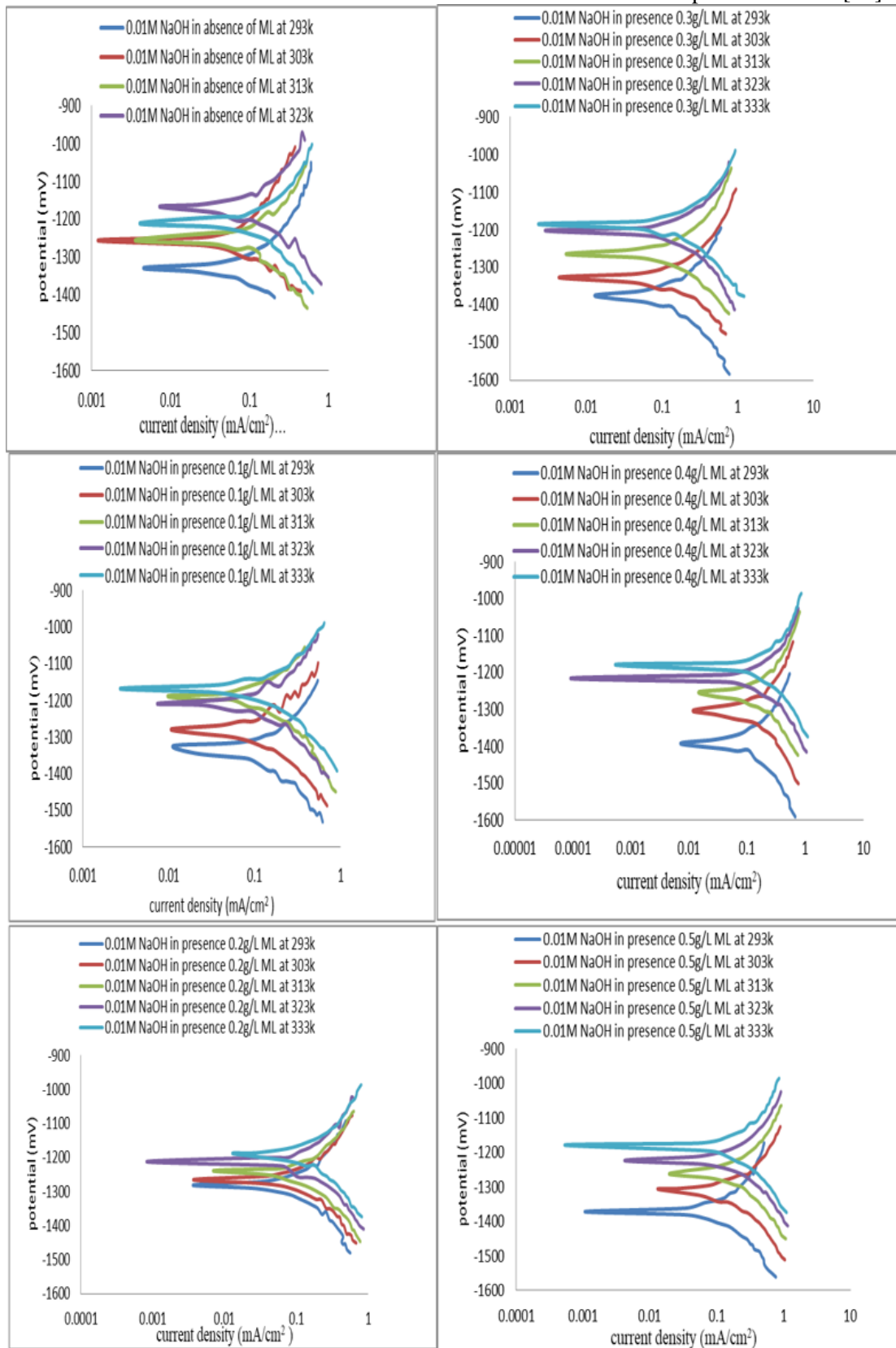


Figure 3-Polarization curves of 7051 aluminum alloy in presence and absence of ML extract at different temperatures.

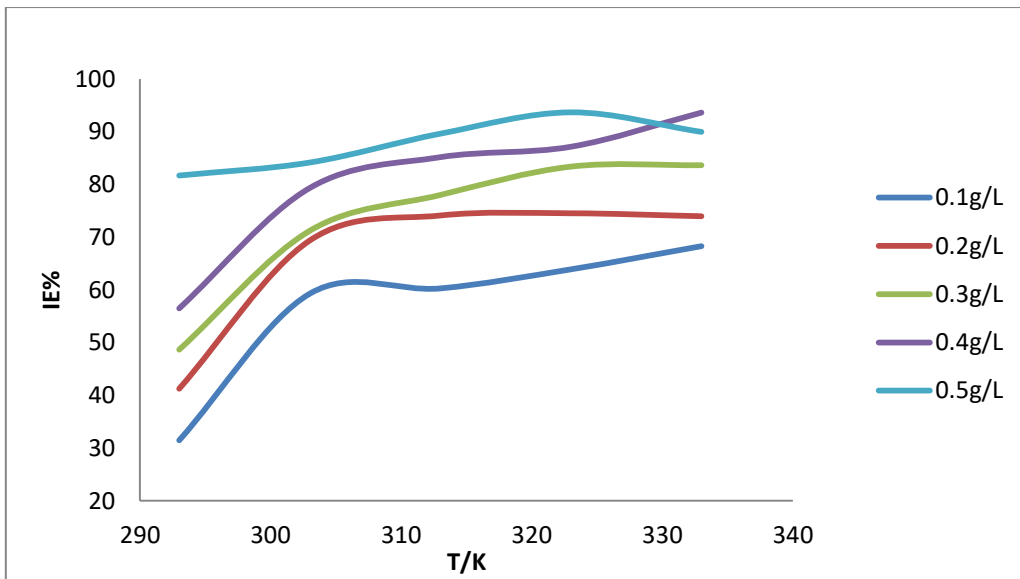


Figure 4-Effects of temperature on the inhibition efficiency of ML in alkaline media.

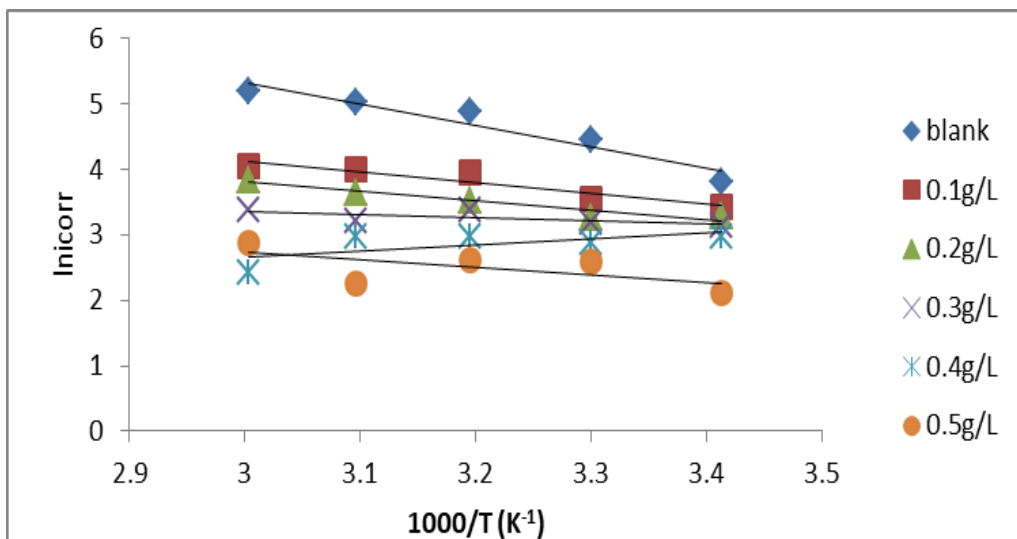


Figure 5-Arrhenius plot results for 7051 aluminum alloy in 0.01M NaOH in presence and absence of ML extract.

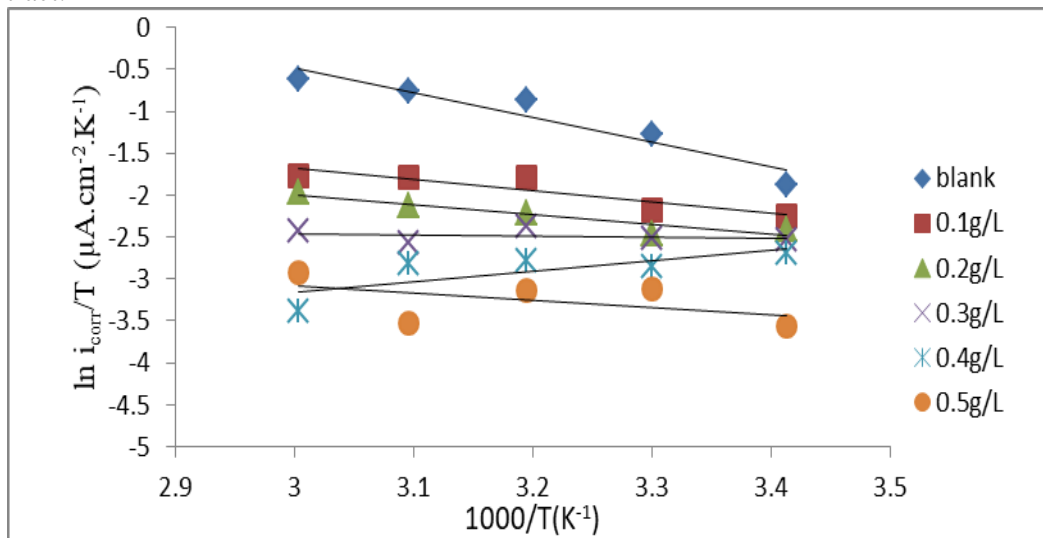


Figure 6- $\ln(I_{corr}/T)$ against $1/T$ for 7051 aluminum alloy in 0.01M NaOH in presence and absence of ML extract.

Table 3-Activation parameters of 7051 aluminum alloy in 0.01M NaOH in presence and absence of ML extract.

Inhibitor conc.(g.L ⁻¹)	E _a (kJ.mol ⁻¹)	ΔH*(kJ.mol ⁻¹)	ΔS*(J.mol ⁻¹ .K ⁻¹)
0.0	27.252	24.658	-127.555
0.1	13.583	10.988	-178.585
0.2	12.157	9.562	-185.500
0.3	3.937	1.342	-213.899
0.4	7.881	10.475	-255.217
0.5	9.725	7.131	-201.757

3.5. Mechanism of inhibition

The milk thistle extract components adsorbed on the aluminum surface, presumably in monolayer thickness, which blocks the aluminum dissolution and H⁺ discharge. Hence, the addition of extract to base solution does not considerably alter the corrosion potential, although the rate of corrosion dramatically decreased.

The main components of milk thistle extract are silybin, isosilybin, silychristin and silydianin, which contain a large and favorable polar group (OH-group), the size, shape, orientation and electric charge of which all participate in inhibition efficiency [16,27]. The increase of inhibition efficiency with temperature is probably because the adsorption increases or the film structure becomes more favorable at high temperature. FTIR measurement (Figure-8) shows shifts in the bands at 3463.92, 3433.06 and 3375.20 cm⁻¹ to 3533.35, 3469.70 and 3438.84 cm⁻¹ respectively. Also, the band at 3413.77 cm⁻¹ disappears, confirming the participation of the OH-group, which is supported by the absence of the N-H group. Table-4 shows the chemical structures of main milk thistle extract compounds.

Table 4-Chemical structure of main milk thistle extract compounds [26, 28].

Constituent	Chemical structure
<p>Silybin</p> <p>IUPAC name: (2R,3R)-3,5,7-trihydroxy-2-[(2R,3R)-3-(4-hydroxy-3-methoxyphenyl)-2-(hydroxymethyl)-2,3-dihydrobenzo[b][1,4]dioxin-6-yl]chroman-4-one</p>	
<p>Isosilybin</p> <p>IUPAC name: 3,5,7-trihydroxy-2-[2-(4-hydroxy-3-methoxyphenyl)-3-(hydroxymethyl)-2,3-dihydro-1,4-benzodioxin-6-yl]-2,3-dihydrochromen-4-one</p>	
<p>Silychristin</p> <p>IUPAC name: (2R,3R)-3,5,7-trihydroxy-2-[(2R,3S)-7-hydroxy-2-(4-hydroxy-3-methoxyphenyl)-3-(hydroxymethyl)-2,3-dihydro-1-benzofuran-5-yl]-2,3-dihydrochromen-4-one</p>	
<p>Silydianin</p> <p>IUPAC name: (1R,3R,6R,7R,10R)-3-hydroxy-10-(4-hydroxy-3-methoxyphenyl)-8-[(2R)-3,5,7-trihydroxy-4-oxo-2,3-dihydrochromen-2-yl]-4-oxatricyclo[4.3.1.0^{3,7}]dec-8-en-2-one</p>	



Figure 7-FTIR spectra: (A) Milk thistle extract and (B) Milk thistle after adsorption on aluminum surface.

4. Conclusions

1. The water extract of milk thistle acts as an admirable inhibitor for corrosion of 7051 aluminum alloy in 0.01 M NaOH media. The raise of the extract quantity present in the alkali solution increased the inhibition efficiency.
2. The inhibition process occurred as a result of adsorption of the milk thistle extract components onto the surface of the 7051 aluminum alloy.
3. This study assumes chemical adsorption on the surface of 7051 aluminum alloy based on increasing the efficiency of inhibition with temperature.
4. The FTIR measurements supported by the chemical structure of the milk thistle extract components showed that the hydroxide group is the main factor in the adsorption process.

References

1. Andrey Drozdov .2007. Aluminium. Thirteenth Element. *Encyclopedia*. 1–231.
2. Armstrong RD. and Braham VJ .1996.The mechanism of aluminium corrosion in alkaline solutions. *Corros Sci* **38**(9): 1463–1471.
3. Noor EA .2009. Potential of aqueous extract of Hibiscus sabdariffa leaves for inhibiting the corrosion of aluminum in alkaline solutions. *J Appl Electrochem*, **39**: 1465–1475.
4. Abiola OK, Otaigbe JOE. and Kio OJ . 2009. Gossipium hirsutum L. extracts as green corrosion inhibitor for aluminum in NaOH solution. *Corros Sci*, **51**: 1879–1881.
5. Al-Moubaraki AH, Al-Howiti AA, Al-Dailami MM, et al.2017. Role of aqueous extract of celery (*Apium graveolens* L.) seeds against the corrosion of aluminium/sodium hydroxide systems. *J Environ Chem Eng*, **5**: 4194–4205.

6. Oguzie EE .2007. Corrosion inhibition of aluminium in acidic and alkaline media by Sansevieria trifasciata extract. *Corros Sci*, **49**: 1527–1539.
7. Abdel-Gaber AM, Khamis E, Abo-ElDahab H, et al. 2008. Inhibition of aluminium corrosion in alkaline solutions using natural compound. *Mater Chem Phys*, **109**: 297–305.
8. Raghavendra N, Hublikar L V., Patil SM, et al.2019. Efficiency of sapota leaf extract against aluminium corrosion in a 3 M sodium hydroxide hostile fluid atmosphere: a green and sustainable approach. *Bull Mater Sci*, **42**: 1–11.
9. Abiola OK. and Otaigbe JOE .2009. The effects of Phyllanthus amarus extract on corrosion and kinetics of corrosion process of aluminum in alkaline solution. *Corros Sci*, **51**: 2790–2793.
10. Nardeli J V., Fugivara CS, Taryba M, et al.2019. Tannin: A natural corrosion inhibitor for aluminum alloys. *Prog Org Coatings*, **135**: 368–381. doi:10.1016/j.porgcoat.2019.05.035
11. The Aluminum Association.2018. International Alloy Designations and Chemical Composition Limits for Wrought Aluminum and Wrought Aluminum Alloys, Arlington.
12. Wysocka J, Cieslik M, Krakowiak S, et al. 2018. Carboxylic acids as efficient corrosion inhibitors of aluminium alloys in alkaline media. *Electrochim Acta*, **289**: 175–192.
13. Saleh KA, Ali MI .2020. Electro polymerization for (N-terminal tetrahydrophthalamic acid) for anti-corrosion and biological activity applications. *Iraqi J Sci*, **61**: 1–12.
14. Hiromoto S .2010. Corrosion of metallic biomaterials, *Metals for Biomedical Devices*, Elsevier, 99–121.
15. Quy Huong D, Duong T. and Nam PC .2019. Effect of the Structure and Temperature on Corrosion Inhibition of Thiourea Derivatives in 1.0 M HCl Solution. *ACS Omega*, **4**: 14478–14489. doi: 10.1021/acsomega.9b01599
16. Chaubey N, Savita, Singh VK, et al. 2017. Corrosion inhibition performance of different bark extracts on aluminium in alkaline solution. *J Assoc Arab Univ Basic Appl Sci*, **22**: 38–44.
17. Al-Rudaini KA .2017. Adsorption Removal of Rhodamine-B Dye from Aqueous Solution Using Rhamnus Stone as Low Cost Adsorbent. *J Al-Nahrain Univ*, **20**: 32–41.
18. Abbas HA, Saleh Alsaade KA. and Yousif Almashhdan HA .2019. Study the effect of cyperus rotundus extracted as mouthwash on the corrosion of dental amalgam, *IOP Conference Series: Materials Science and Engineering*, 1–11.
19. Kareem KA.2017. Equilibrium and kinetic studies of Gentian Violent Dye Adsorption onto Activated carbon prepared from Aldhanan Hull. *Al-Mustansiriyah J Sci*, **28**: 89–96.
20. Zhang J, Klasky M. and Letellier BC .2009. The aluminum chemistry and corrosion in alkaline solutions. *J Nucl Mater*, **384**: 175–189.
21. Khadraoui A, Khelifa A. and Hadjmelianni M, et al. 2016. Extraction, characterization and anti-corrosion activity of Mentha pulegium oil: Weight loss, electrochemical, thermodynamic and surface studies. *J Mol Liq*, **216**: 724–731.
22. Ostovari A, Hoseinie SM. and Peikari M, et al.2009. Corrosion inhibition of mild steel in 1 M HCl solution by henna extract: A comparative study of the inhibition by henna and its constituents (Lawsone, Gallic acid, α -d-Glucose and Tannic acid). *Corros Sci*, **51**: 1935–1949.
23. Fouda AS, El-shereafy EE, Hathoot AA, et al. 2020. Corrosion Inhibition of Aluminum by Cerium rubrum Extract in Hydrochloric Acid Environment. *J Bio- Tribo-Corrosion*, **6**: 37.
24. Almashhadani HA, Saleh KA.2019. Corrosion protection of pure titanium implant by electrochemical deposition of hydroxyapatite post-anodizing, *IOP Conference Series: Materials Science and Engineering*, 1–9.
25. Kubba RM, Al-Majidi SMH, Ahmed AH.2019. Synthesis, characterization and quantum chemical studies of inhibition ability of novel 5-nitro isatin derivatives on the corrosion of carbon steel in sea water. *Iraqi J Sci*. **60**: 688–705.
26. Soltani N, Tavakkoli N, Khayat Kashani M, et al. 2014. Silybum marianum extract as a natural source inhibitor for 304 stainless steel corrosion in 1.0M HCl. *J Ind Eng Chem*, **20**: 3217–3227.
27. Kareem KA.2017. Equilibrium, kinetic and thermodynamics studies of lead Adsorption from Aqueous Solution onto Activated carbon prepared from Silybum mairanum. *Int J chem tech Res*, **10**: 760–766.
28. Kim NC, Graf TN, Sparacino CM, et al. 2003. Complete isolation and characterization of silybins and isosilybins from milk thistle (Silybum marianum). *Org Biomol Chem*, **1**: 1684–1689.